Journal of Solid State Chemistry **144,** 152–158 (1999)
Article ID jssc.1999.8135, available online at http://www.idealibrary.com on IDEAL®

Crystal Structures of $U(Ta,W)_5O_{16}$ and $U(Ta,W)_2O_8$ Revealed by High-Resolution Transmission Electron Microscopy

Charlotta Askeljung and Margareta Sundberg

Department of Inorganic Chemistry, Arrhenius Laboratory, Stockholm University, S-106 91 Stockholm, Sweden

Received July 8, 1998; in revised form December 7, 1998; accepted December 10, 1998

Two new phases, $U(Ta,W)_5O_{16}$ and $U(Ta,W)_2O_8$, were formed by solid state reaction of the binary oxides (U_3O_8, Ta_2O_5, and WO_3) and Ta metal powder. They were characterized by high-resolution transmission electron microscopy and X-ray powder diffraction techniques. The phases are orthorhombic with the following unit cell dimensions: $U(Ta,W)_5O_{16}$, $a = 10.052(1)$, $b = 7.3207(5)$, and $c = 7.9600(4)$ Å; and $U(Ta,W)_2O_8$, $a = 20.232(2)$, $b = 7.4520(4)$, and $c = 4.0652(2)$ Å. Both structures are built up of $(Ta,W)O_6$-octahedra arranged as ReO_3-type slabs two octahedra wide. In $U(Ta,W)_5O_{16}$ these slabs are connected by a thin lamella consisting of hexagonal UO_8-bipyramids and $(Ta,W)O_6$-octahedra alternating along both the b and c axes. EDS analysis indicated a composition of $UTa_{1.5}W_{3.5}O_{16}$. The structure is related to UMo_5O_{16}, but with every other layer displaced through $\frac{1}{2}b$. The second phase, $U(Ta,W)_2O_8$, is isotypic with the orthorhombic modification of UMo_2O_8, in which the ReO_3-type slabs are intergrown with lamellas of edge-sharing pentagonal UO_7-bipyramids. The composition $UTa_{0.5}W_{1.5}O_8$ was obtained by EDS analysis. Some defects in terms of three-octahedra-wide ReO_3-type slabs have been observed in $U(Ta,W)_5O_{16}$ crystals. EDS analyses of such crystals showed a high-tungsten and a low-tantalum content. © 1999 Academic Press

INTRODUCTION

As a part of a project concerning structural characterization at the atomic level of L-Ta_2O_5 related phases by high-resolution transmission electron microscopy (HRTEM), it was considered profitable to investigate the formation of U_3O_8– and L-Ta_2O_5 related phases in the system U_3O_8–UO_2–Ta_2O_5–WO_3. This system was selected partly because L-Ta_2O_5 related phases, both commensurate and incommensurate, are formed in the subsystem Ta_2O_5–WO_3 (1–5), and partly because the L-Ta_2O_5 structure may be considered as related to both α- and β-U_3O_8 (6,7) and to α-UO_3 (2). Few data are available concerning the phases formed in the quaternary system.

In 1975, Baud *et al.* (8) investigated some samples with composition $U_{x/4}(Ta_xW_{1-x})O_3$. They observed three tungsten bronze related phases: one tetragonal with unit cell dimensions $a = 5.285$ and $c = 3.832$ Å in the region $0 < x/4 < 0.05$, one cubic with $a = 3.788$–3.848 Å, for $0.05 < x/4 < 0.15$, and another tetragonal with $a = 7.704$–7.745 and $c = 3.854$–3.885 Å for $0.16 < x/4 < 0.25$.

In the present paper, we report the existence of two new complex U-(Ta,W)-oxides. These compounds were found by HRTEM studies of $U_{x/4}(Ta_xW_{1-x})O_3$ ($x = 0.4$) and some other samples prepared in the system above. The structures of these oxides were deduced from HRTEM images and verified by simulated image calculations. Both ordered and defect structures will be presented below.

EXPERIMENTAL

Samples of compositions $UTa_4W_6O_{30}$, $UTa_2W_3O_{16}$, $UTa_3W_2O_{16}$, $U_2TaW_3O_{16}$, and $UTaWO_8$ were prepared by mixing appropriate amounts of U_3O_8 (prepared by heating $UO_2(NO_3)_2 \cdot 6\,H_2O$ at 970 K), Ta_2O_5, WO_3, and Ta-metal powder. After mixing and grinding the oxides and the metal, the mixtures were heated in evacuated sealed silica tubes and held at 970 K for 10 h, then at 1370 and 1320 K for 3 and 14 days, respectively, and were finally slowly cooled in the furnace.

X-ray powder diffraction patterns were registered in a Guinier–Hägg focusing camera with monochromatized Cu$K\alpha_1$ radiation, and with Si as internal standard. Unit-cell parameters were refined from the X-ray powder data with the program PIRUM (9), using least-square methods.

The electron microscopy specimens were prepared by crushing small amounts of the samples in an agate mortar under *n*-butanol. Then a few drops of the resultant suspension were allowed to dry on a perforated carbon film supported by a copper grid. A JEOL 2000 FX-II transmission electron microscope, equipped with a LINK QX200 X-ray microanalysis system, was used for selected-area electron diffraction (SAED) studies in combination with energy dispersive spectroscopy (EDS) analysis on the same fragment. The results are based on the U(M), Ta(M), and W(L) lines in the spectra.

0022-4596/99 $30.00

The HRTEM studies of thin crystal fragments were performed in a JEOL 200CX transmission electron microscope, which was equipped with a top-entry goniometer stage, with tilt angles of $\pm 10^\circ$. The microscope was operated at 200 kV, and the radius of the objective aperture used corresponded to 0.41 $Å^{-1}$ in reciprocal space. A few samples were also examined in a JEOL JEM-3010 transmission electron microscope, equipped with a double-tilt side-entry goniometer stage with tilt angles ± 10–20° and operated at 300 kV. The radius of the objective aperture used corresponded to 0.68 $Å^{-1}$ in reciprocal space. Theoretical HRTEM images were calculated with a modified PC version of the SHRLI suite of programs (10).

RESULTS AND DISCUSSION

All products were microcrystalline and of black to dark-gray color. The X-ray powder diffraction patterns and the electron microscopy studies showed that multi-phase samples had been formed. A phase with the pseudo-hexagonal lattice dimensions $a = 7.4$ and $c = 15.7$ Å could be identified in most of the samples. This phase seemed to be related to UTa_3O_{10} (11).

A. $U_x(Ta,W)O_3$, ($x \approx 0.1$), and $U(Ta,W)_5O_{16}$

The SAED patterns of thin fragments from $UTa_4W_6O_{30}$ showed that part of the sample consisted of a tungsten bronze related phase of perovskite type. Some of the lines in the X-ray powder diffraction pattern could be indexed on the basis of a cubic cell with $a = 3.8238(1)$ Å. EDS analyses of nine individual fragments gave an average U:Ta:W ratio of 1:3:6. This compound is related to the cubic phase $U_{x/4}(Ta_xW_{1-x})O_3$, with $x/4 = 0.08$, which has been reported by Baud *et al.* (8).

A few fragments of a tetragonal tungsten bronze (TTB) related phase, containing tantalum and tungsten with Ta:W = 40:60 at.% according to EDS-analysis, were also observed. Some lines in the X-ray powder pattern were identified as originating from a TTB-related phase with unit cell dimensions $a = 12.26$ and $c = 3.886$ Å. Such a compound has been reported in the subsystem Ta_2O_5–WO_3 (12).

The X-ray powder diffraction and electron microscopy studies furthermore revealed the existence of a new phase with unit-cell dimensions $a = 10.052(1)$, $b = 7.3207(5)$, and $c = 7.9600(4)$ ($= 2 \times 3.980$) Å. Figure 1a shows the HRTEM image with the corresponding SAED pattern inserted. The image was taken from a thin crystal fragment aligned with the c axis parallel to the electron beam. The image was recorded close to Scherzer conditions, which means that the metal atoms in projection can be seen as black spots. The HRTEM image in Fig. 1b, on the other hand, was taken at a defocus value where the projected metal atoms yield white contrast. Images consisting of double rows of black and white dots (marked by A in Figs. 1a and 1b, respectively), are characteristic of ReO_3-type slabs two octahedra wide in the structure. The rows of dark dots (marked by arrows) in between the slabs (A) can be interpreted as corresponding to an ordered arrangement of projected U and M (M = Ta,W) atoms in hexagonal UO_8-bipyramids and MO_6-octahedra. The structure model, deduced from HRTEM images, is shown in Figs. 1c and 1d and corresponds to a composition of $U(Ta,W)_5O_{16}$. The EDS data gave the average ratio U:Ta:W = 17:23:60 at.%, which indicates a composition close to $UTa_{1.5}W_{3.5}O_{16}$, ($U(Ta,W)_5O_{16}$).

The electron microscopy results showed that the structure of the new U-(Ta,W)-oxide is closely related to those of the complex uranium–molybdenum-oxides $U_{1-x}Mo_5O_{16}$ ($0 \le x \le 0.5$) (13–16), which have a basic framework structure consisting of ReO_3-type slabs with tilted MoO_6-octahedra, infinite in two dimensions and two octahedra wide in the third as can be seen in Fig. 1e. In UMo_5O_{16}, the ReO_3-type slabs are linked by additional MoO_6-octahedra arranged so that six-sided tunnels are formed. The tunnels are filled by –O–U–O–U–O– atom strings, resulting in eight-coordination of uranium in hexagonal UO_8-bipyramids. The unit cell parameters given above for $U(Ta,W)_5O_{16}$ are similar to those reported for UMo_5O_{16}: $a = 9.885$, $b = 7.167$, and $c = 4.133$ Å (15), except for the c-axis, which is doubled.

The suggested structure model for $U(TaW)_5O_{16}$ (Figs. 1c and 1d) is related to that of UMo_5O_{16}. If every other layer in UMo_5O_{16} (Fig. 1e) is displaced along the b axis by $b/2$, the $U(TaW)_5O_{16}$ structure is formed. This new model still consists of ReO_3-type slabs, two octahedra wide, which are linked by thin lamellas of hexagonal UO_8-bipyramids and octahedra. In $U(TaW)_5O_{16}$, there is an ordered arrangement of hexagonal UO_8-bipyramids (HB) and $(Ta,W)O_6$-octahedra along both the b and c axes. It should be mentioned that UMo_5O_{16} type structures have previously been denoted (n)-HB (13), where n represents the number of octahedra across the ReO_3-type slab. Since the width of the ReO_3-slabs is two octahedra ($n = 2$) in $U(TaW)_5O_{16}$, and the structure contains hexagonal UO_8-bipyramids (HB), it can still be considered to belong to the (2)-HB type structures.

Theoretical HRTEM images of the two structure models $U(Ta,W)_5O_{16}$ (Figs. 1c and 1d) and UMo_5O_{16} (Fig. 1e) have been calculated for different crystal thicknesses and defocus values. The latter calculations were based on the atomic coordinates obtained from a single-crystal X-ray study of the UMo_5O_{16} structure (15) but with Ta substituted for Mo. The parameters used in the calculations of the $U(Ta,W)_5O_{16}$ structure in Figs. 1c and 1d, were based on those for the UMo_5O_{16} structure, modified to suit the suggested model with hexagonal UO_8-bipyramids and TaO_6-octahedra alternating along the c axis. Tungsten was

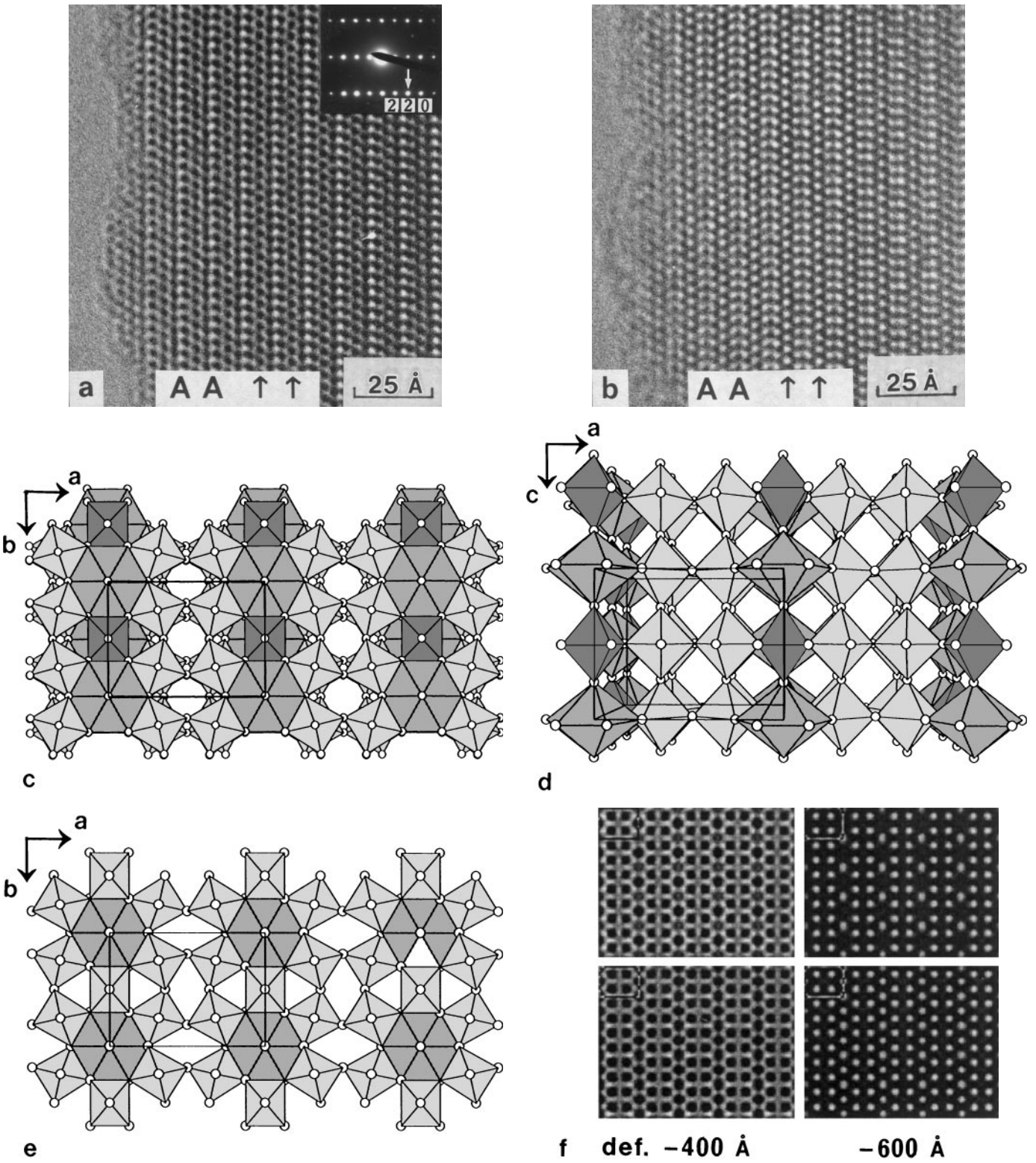

FIG. 1. (a) HRTEM image of $U(Ta,W)_5O_{16}$ projected along [001], with the corresponding SAED-pattern inserted (defocus value ≈ -500 Å). The ReO_3-type slabs are marked A. (b) HRTEM image of the same crystal fragment at a defocus value of ≈ -800 Å. (c) The crystal structure of $U(Ta,W)_5O_{16}$ in [001] and (d) [010] projections. (e) The crystal structure of UMo_5O_{16} in [001] projection. (f) Simulated HRTEM images of UMo_5O_{16} (top) and $U(Ta,W)_5O_{16}$ (bottom), crystal thickness ≈ 40 Å. The drawings are produced with ATOMS by Shape Software.

substituted for molybdenum in the ReO_3-type slabs. The simulated images of UMo_5O_{16} (top) and $U(Ta,W)_5O_{16}$ (bottom) in Fig. 1f show that it is very difficult to distinguish between the two structure models from the black contrast features in HRTEM images taken close to Scherzer focus (-400 Å). However, it should be possible to select a model from the contrast features in HRTEM images taken at a defocus where the projected metal atoms are imaged as white dots. There is good agreement between the recorded HRTEM image (Fig. 1b) and the calculated image at a defocus value of -600 Å in Fig. 1f, which supports the suggested structure with an ordered arrangement of uranium and tantalum atoms along the *c* axis.

In order to find and confirm the composition range for the new compound, a few samples with different U:Ta:W ratios were synthesized. Large amounts of the $U(Ta,W)_5O_{16}$ phase were found in the two samples $UTa_2W_3O_{16}$ and $U_2TaW_3O_{16}$. The unit-cell dimensions refined from the X-ray powder pattern of $UTa_2W_3O_{16}$ were almost identical to those given above for $UTa_{1.5}W_{3.5}O_{16}$. The composition was also confirmed by microanalysis. On the other hand, EDS analyses of $U(Ta,W)_5O_{16}$ fragments from the $U_2TaW_3O_{16}$ sample indicated that U:Ta:W $\approx$ 18:7:75 at.%, showing a higher tungsten content in these crystals. A small decrease in the refined unit-cell dimensions was also observed. The HRTEM study indicated defects in the crystals, which to some extent could explain the variation in composition. These defects will be discussed below.

B. $U(Ta,W)_2O_8$

Electron microscopy studies of the $UTaWO_8$ and $UTa_3W_2O_{16}$ samples revealed a second new phase with an average U:(Ta,W) ratio of 1:2. The SAED pattern shown in Fig. 2a, the contrast features in the corresponding HRTEM image in Fig. 2b, and the EDS result suggested that the new U-(Ta,W) oxide is isotypic with the orthorhombic modification of UMo_2O_8 (17). As in the previous HRTEM image of $U(Ta,W)_5O_{16}$, shown in Fig. 1a, the parallel slabs of dark spots in Fig. 2b (marked by A) correspond to ReO_3-like regions, two MO_6-octahedra wide (M = Ta,W) in the structure. The zigzag arrangement of black dots (marked by arrows in Fig. 2b) separating the slabs in this case represents projected uranium atoms in pentagonal UO_7 bipyramids. The structure model of $U(Ta,W)_2O_8$ shown in Fig. 2c can be described as built up of ReO_3-type slabs of tilted octahedra, two $(Ta,W)O_6$-octahedra wide ($n = 2$), which are intergrown with thin slabs of edge-sharing pentagonal UO_7 bipyramids (PB). This type of structure has previously been denoted (2)-PB (13). From the SAED pattern (Fig. 2a) approximate lattice constants were calculated to be $a \approx 20.1$ and $b \approx 7.4$ Å. The X-ray powder data of the $UTaWO_8$ sample could be indexed with a unit cell of orthorhombic symmetry and with $a = 20.232(2)$, $b = 7.4520(4)$, and $c = 4.0652(2)$ Å. These values are fairly close to those previously reported for the UMo_2O_8 (orth.) compound; $a = 20.076$, $b = 7.323$, and $c = 4.116$ Å (17). EDS analyses of

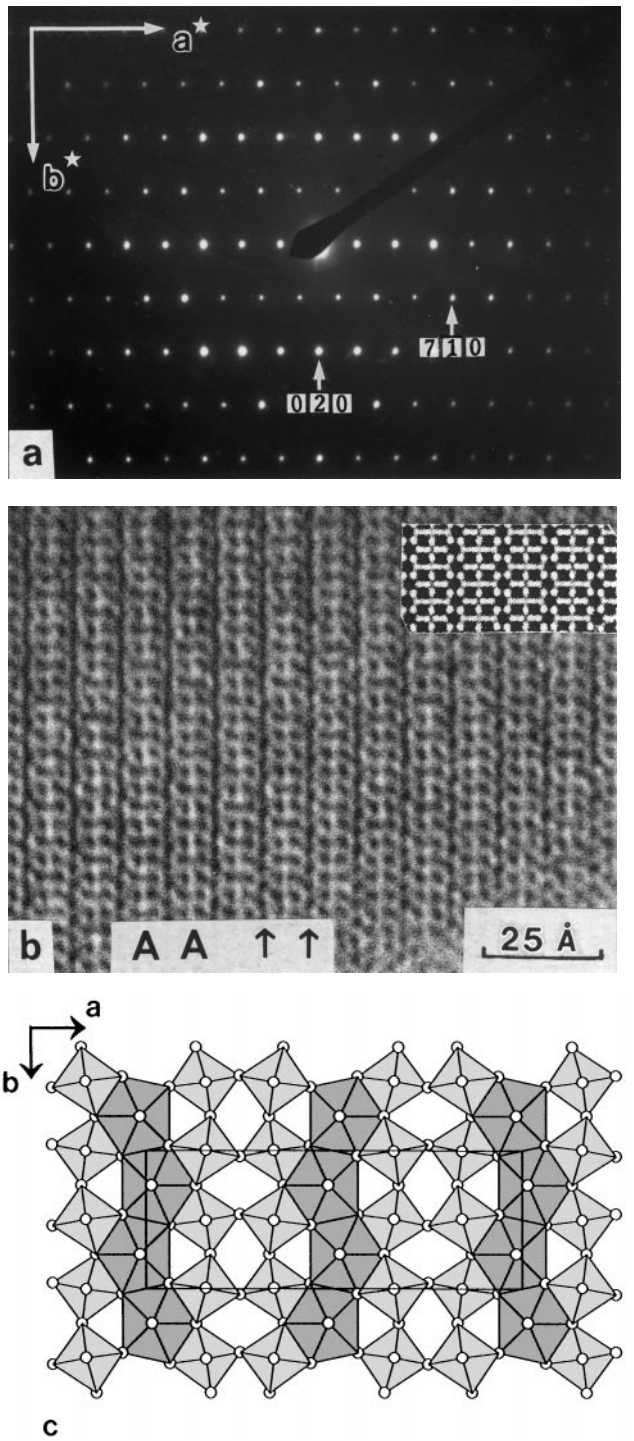

FIG. 2. (a) SAED-pattern of $U(Ta,W)_2O_8$ ([001] zone). (b) The corresponding HREM-image with a simulated image inserted, crystal thickness 20 Å and defocus value -500 Å. (c) The crystal structure of $U(Ta,W)_2O_8$ projected along the *c* axis. The drawing is produced with ATOMS by Shape Software.

crystals from the $UTaWO_8$ sample gave U:Ta:W ≈ 33:22:45 at.%, suggesting a composition of $UTa_{0.6}W_{1.4}O_8$ for the $U(Ta,W)_2O_8$ phase, whereas microanalyses of fragments from the $UTa_3W_2O_{16}$ samples resulted in a somewhat higher W/Ta ratio. No defects have been found so far.

Theoretical HRTEM images were calculated for different crystal thicknesses and defocus values. The calculations were based on the atomic parameters of UMo_2O_8 (orth.) given by Cremers *et al.* (17) and with Ta substituted for Mo. The theoretical image inserted in Fig. 2b agrees fairly well with the HRTEM image. The small differences in contrast features indicate that the $(Ta,W)O_6$ octahedra in $U(Ta,W)_2O_8$ are slightly more distorted than the corresponding MoO_6 octahedra in the UMo_2O_8 structure.

The HRTEM images taken of $U(Ta,W)_5O_{16}$ (Fig. 1a) and $U(Ta,W)_2O_8$ (Fig. 2b) crystals are very similar in appearance and therefore cannot be used for structure discrimination. But the two compounds can easily be identified from their SAED patterns in [001] projection, as seen in Figs. 1a and 2a. This is in agreement with previous results obtained for complex uranium–molybdenum oxides (13).

It is interesting to note that the structure of $UTa_{0.5}W_{1.5}O_8$ is different from those of UTa_2O_8 (18) and $U(WO_4)_2$ (19). UTa_2O_8 is reported to have hexagonal unit-cell dimensions $a = 6.410$ and $c = 3.950$ Å. $U(WO_4)_2$ is isostructural with $Th(MoO_4)_2$ (20), and the uranium atoms are eight-coordinated by distorted square antiprisms which share oxygen corner atoms with WO_4-tetrahedra. In a recent HRTEM study of the subsystem UO_2–WO_3 (19), only a few isolated defects of UW_2O_8 with a (2)-PB type structure were observed to be intergrown with an ordered (3)-PB type structure of UW_3O_{11}. The present study has shown that a 20–35 at.% replacement of W by Ta in $U(WO_4)_2$ creates a $UTa_xW_{2-x}O_8$ phase ($x \approx 0.5$–0.6) which adopts

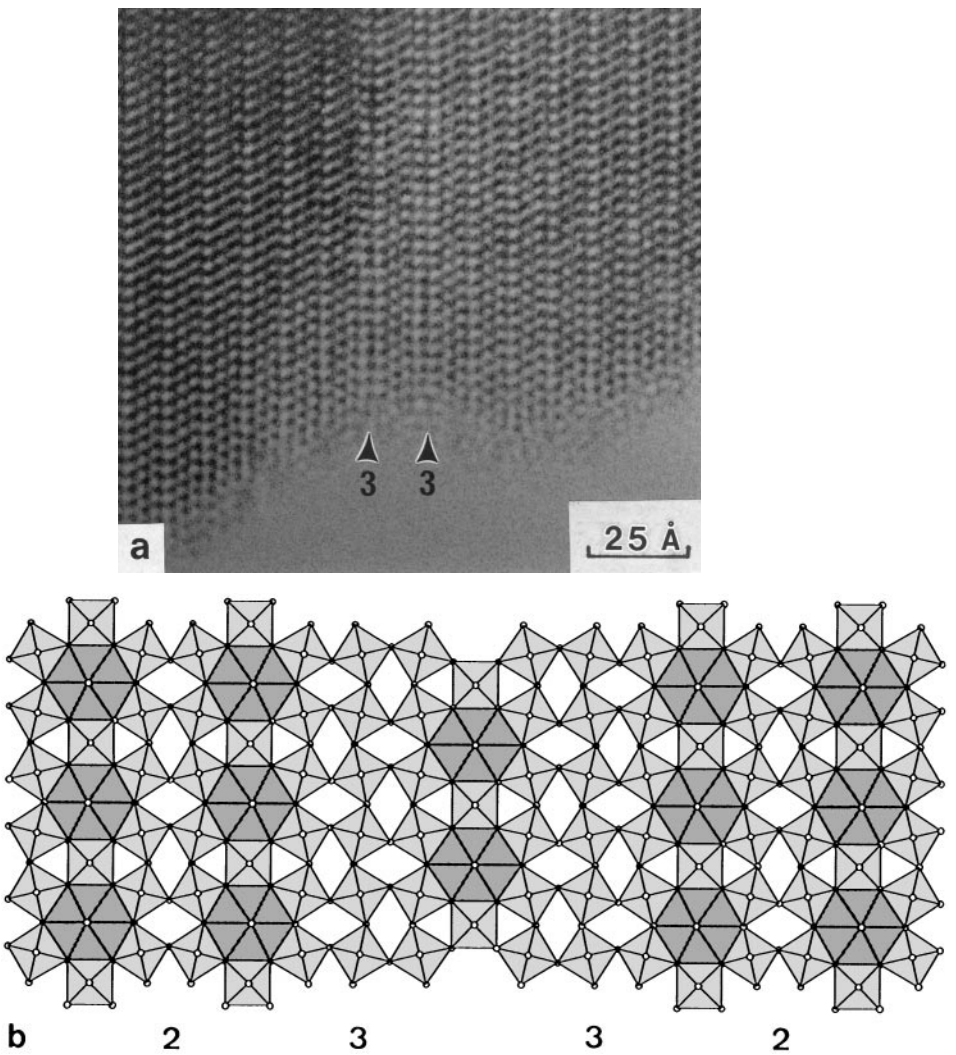

FIG. 3. (a) HRTEM image of a thin crystal of $U(Ta,W)_5O_{16}$ in [001] projection, showing defects marked by arrows. (b) One layer of the corresponding idealized structure model. The drawings are produced with ATOMS by Shape Software.

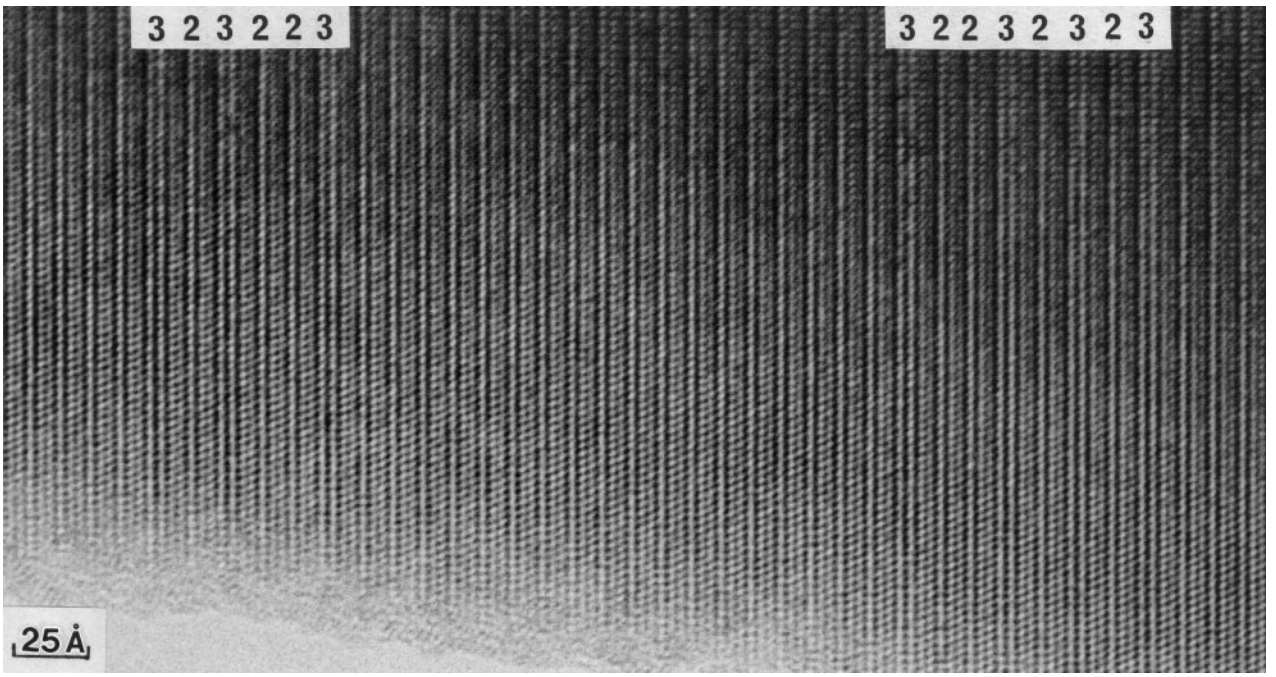

FIG. 4. HRTEM image of a thin crystal of $U(Ta,W)_5O_{16}$ in [001] projection, showing a large area of ReO_3-type slabs three octahedra wide.

the UMo_2O_8 (orth.) structure. Similar results have been reported in the subsystem UMo_2O_8–UW_2O_8 (21), where there exists an extended $U(Mo_{1-x}W_x)_2O_8$ (orth.) solid solution up to $x = 0.7$.

C. Defects

Structural defects in the form of isolated slabs of ReO_3 type, three octahedra wide, were seen in some $U(Ta,W)_5O_{16}$ crystals from the bulk sample $U_2TaW_3O_{16}$. The HRTEM image in Fig. 3a, with the corresponding structure model in Fig. 3b, shows that two adjacent ReO_3 slabs of width $n = 3$ are intergrown with the $U(Ta,W)_5O_{16}$ structure ((2)-HB type). It is interesting to note that those two ReO_3 slabs together correspond to a thin lamella, one unit cell wide, of the (3)-HB type structure. The stoichiometric formula of such a compound with full occupancy of all atom positions is $U(Ta,W)_7O_{22}$. No ordered fragment or large region of the (3)-HB type structure has been observed so far in the system. A phase of this structure type, $U_{0.5}Mo_{3.3}W_{3.7}O_{22}$, with half occupancy of the uranium positions has been reported, however (13).

The HRTEM image in Fig. 4 shows a large disordered region where every second or third ReO_3-type slab has a width of three octahedra. The presence of these wide slabs in some crystals indicate that they have high-tungsten and low-tantalum content, as tungsten is known to enter and stabilize the ReO_3-type slabs. The defect-rich crystals were all taken from samples with high-tungsten and low-tantalum contents in the initial composition, and a high-tungsten content was also confirmed by the EDS analysis. It should be mentioned that ReO_3-type slabs with $n > 3$ have not yet been observed in the $U(Ta,W)_5O_{16}$ crystals. The above results are in analogy with previous observations that substitution of tungsten for molybdenum increases the width of the ReO_3-type slabs both in complex U–Mo–W oxides (13) and in ternary mixed Mo–W oxides, such as the $\{102\}$-crystallographic shear structures $(Mo,W)_nO_{3n-1}$, $10 \leq n \leq 14$ (22), and the two Mo_4O_{11}-type related phases $(Mo,W)_7O_{25}$ (mon) (23) and $(Mo,W)_7O_{25}$(orth.) (24).

CONCLUDING REMARKS

It has been shown above that both $U(Ta,W)_5O_{16}$ with a (2)-HB type structure and $U(Ta,W)_2O_8$ with a (2)-PB type structure are formed. The first type of structure is observed in samples with starting compositions $UTa_4W_6O_{30}$ and $UTa_2W_3O_{16}$, and the other structure is found in the bulk samples $UTa_3W_2O_{16}$ and $UTaWO_8$. $U(Ta,W)_5O_{16}$ is formed when $W/Ta > 1$ in the starting material, whereas $U(Ta,W)_2O_8$ is formed when $W/Ta \leq 1$. It is also worth mentioning that the U content in the $U(Ta,W)_2O_8$ structure is twice as high as in $U(Ta,W)_5O_{16}$. Defects of the (3)-HB type structure are frequently observed in crystals from the sample $U_2TaW_3O_{16}$ which has $W/Ta > 1$.

ACKNOWLEDGMENTS

We thank Dr. B.-O. Marinder for valuable comments on the manuscript. We are also grateful to Mrs. Jaroslava Östberg for technical assistance with the photographic work. This investigation forms part of a research project financially supported by the Swedish Natural Science Research Council.

REFERENCES

1. N. C. Stephenson and R. S. Roth, *Acta Crystallogr., Sect. B* **27,** 1037 (1971).
2. S. Schmid, R. L. Withers, and J. G. Thompson, *J. Solid State Chem.* **99,** 226 (1992).
3. S. Schmid, J. G. Thompson, A.D. Rae, B.D. Butler, and R.L. Withers, *Acta Crystallogr., Sect. B* **51**, 698 (1995).
4. A. D. Rae, S.Schmid, J. G. Thompson, and R. L. Withers, *Acta Crystallogr., Sect. B* **51,** 709 (1995).
5. T. Miyano, *J. Solid State Chem.* **126,** 208 (1996).
6. G. Harburn, R. J. D. Tilley, J. M. Williams, and R. P. Williams, *J. Chem. Soc. Faraday Trans.* **88,** 621 (1992).
7. G. Harburn, R. J. D. Tilley, and R. P. Williams, *Philos. Mag.*, [*Part*] *A* **68,** 633 (1993).
8. G. Baud, R. Sabatier, J. Y. Feneyrol, and M. Capestan, *J. Inorg. Nucl. Chem.* **37,** 101 (1975).
9. P.-E. Werner, *Ark. Kemi.* **31,** 513 (1969).
10. M. A. O'Keefe, P. R. Buseck, and S. Iijima, *Nature* (*London*), **274,** 322 (1978).
11. R. Chevalier and M. Gasperin, *C. R. Acad. Sci. Paris, Series C* **265,** 1101 (1967).
12. L. M. Kovba and V. K. Trunov, *Proc. Acad. Sci. USSR* (*Chem. Sec.*) **147,** 1015 (1963).
13. M. Sundberg and V. Tabachenko, *Microsc. Microanal. Microstruct.* **1,** 373 (1990).
14. M. Sundberg and B.-O. Marinder, *Eur. J. Solid State Inorg. Chem.* **31,** 855 (1994).
15. V. V. Tabachenko, O. G. D'Yachenko, and M. Sundberg, *Eur. J. Solid State Inorg. Chem.* **32,** 1137 (1995).
16. M. Sundberg, "Proc. 13th. Int. Congress of Electron Microscopy Paris, 1994," Vol. 1, p. 955.
17. T. L. Cremers, P. G. Eller, R. A. Penneman, and C. C. Herrick, *Acta Crystallogr., C* **39,** 1163 (1983).
18. M. Gasperin, *Bull. Soc. Franc. Minér. Crist.* **83,** 1 (1960).
19. M. Sundberg and B.-O. Marinder, *J. Solid State Chem.* **121,** 167 (1996).
20. T. L. Cremers, P. G. Eller, and R. A. Penneman, *Acta Crystallogr., Sect. C* **39,** 1165 (1983).
21. O. N. Rozanova, L. M. Kovba, and V. K. Trunov, *Vestn. Mosk. Univ. Ser. 2 Khim.* **23,** 100 (1968).
22. A. Magnéli, B. Blomberg-Hansson, L. Kihlborg, and G. Sundkvist, *Acta Chem. Scand.* **9,** 1382 (1955).
23. F. Portemer, M. Sundberg, L. Kihlborg, and M. Figlarz, *J. Solid State Chem.* **103,** 403 (1993).
24. L. Kihlborg, B.-O. Marinder, M. Sundberg, F. Portemer, and O. Ringaby, *J. Solid State Chem.* **111,** 111 (1994).